Comparative Biochemistry and Physiology, Part C 255 (2022) 109293

Contents lists available at ScienceDirect

Comparative Biochemistry and Physiology, Part C

journal homepage: www.elsevier.com/locate/cbpc

Metabolite features and oxidative response in kidney of red crucian carp (*Carassius auratus* red var) after *Aeromonas hydrophila* challenge

Ning-Xia Xiong [a,1], Zhuang-Wen Mao [b,1], Jie Ou [a], Lan-Fen Fan [c], Yuan Chen [a,b], Sheng-Wei Luo [a,*], Kai-Kun Luo [a], Ming Wen [a], Shi Wang [a], Fang-Zhou Hu [a], Shao-Jun Liu [a,*]

[a] State Key Laboratory of Developmental Biology of Freshwater Fish, College of Life Science, Hunan Normal University, Changsha 410081, PR China
[b] Hunan Provincial Key Laboratory of Nutrition and Quality Control of Aquatic Animals, Department of Biological and Environmental Engineering, Changsha University, Changsha 410022, PR China
[c] College of Marine Sciences, South China Agricultural University, Guangzhou, 510642, PR China

ARTICLE INFO

Edited by Martin Grosell

Keywords:
Crucian carp
Metabolomics
Aeromonas hydrophila
Oxidative stress

ABSTRACT

Aeromonas hydrophila can threaten the survival of freshwater fish. In this study, *A. hydrophila* challenge could induce tissue damage, promote antioxidant imbalance as well as alter the transcript levels of oxidative stress indicators, apoptotic genes and metabolic enzyme genes in kidney of red crucian carp (RCC). Metabolomics analysis revealed that *A. hydrophila* challenge had a profound effect on amino acid metabolism and lipid metabolism. In addition, we further identified dipeptides, fatty acid derivatives, cortisol, choline and tetrahydrocortisone as crucial biomarkers in kidney of RCC subjected to *A. hydrophila* infection. These results highlighted the importance of metabolic strategy against bacterial infection.

1. Introduction

Increasing evidences have demonstrated that exposure to environmental hazards may result in pathogenesis of severe diseases in mammals [1]. Similarly, both biotic and abiotic stressors can cause physiological malfunction and immune dysregulation in fish, rendering fish more susceptible to invading pathogens [2,3]. Additionally, the release of pollutants, including antibiotics and heavy metals, may promote the increasing numbers of resistant bacteria [4,5].

Microbial diseases can threaten the survival of aquatic animals, causing a great economic loss [6]. Crucian carp (*Carassius auratus*) is one of the most important economic freshwater fish and abundant in lakes, rivers and reservoirs in China, which is popular with fish farmers [7]. However, accumulating reports have pointed out that *A. hydrophila* may be the dominant motile *Aeromonas* species that causes disease outbreaks in aquaculture [8]. Invading pathogens successfully breach mucosal and epithelial barriers that can cause inflammatory events, whilst a large range of cell types and signal mediators are involved in pathogen-induced inflammatory response [9]. In addition, bacterial infection and endotoxin stimulation may stimulate the generation of reactive oxygen species (ROS) in aquatic animals [10,11]. Antioxidant enzymes and endogenous antioxidants can serve as the first cellular defense agaisnt oxidative stress, but ROS accumulation may exhibit an adverse effect on the organisms, triggering antioxidant imbalance and lipid peroxidation [12]. *A. hydrophila* is a gram-negative pathogen capable of generating various virulence factors, which is a widespread representative of *Aeromonadaceae* found in water, river sediment, fish and shellfish [13]. Previous studies have demonstrated that *A. hydrophila* infection can significantly increase accumulative mortality of allogynogenetic crucian carp at the doses of 1×10^8 CFU ml^{-1} [14].

Although immunoprophylaxis is an effective strategy in the spread limitation of pathogenic infection [15], vaccine application cannot always deal with all issues of infectious diseases and antibiotics bioaccumulation, which may easily trigger the emergence of antibiotic resistance bacteria (ARB) in water environment [16]. Immunometabolism is an emerging field of investigation linking immunolgy to metabolism, which has emerged as an important mechanism central to innate and adaptive immune regulation and provided a new insight into the underlying mechanism between infection-induced systemic inflammation and homeostasis [17].

In this study, the aims were to evaluate the antioxidant status and metabolite profiles of red crucian carp (RCC, *Carassius auratus* red var).

* Corresponding authors.
E-mail addresses: swluo@hunnu.edu.cn (S.-W. Luo), lsj@hunnu.edu.cn (S.-J. Liu).
[1] These authors contributed equally to this work.

https://doi.org/10.1016/j.cbpc.2022.109293
Received 5 December 2021; Received in revised form 12 January 2022; Accepted 30 January 2022
Available online 4 February 2022

This study may provide a comprehensive data on the biochemical pathways and immunometabolic status of *A. hydrophila*-infected fish.

2. Materials and methods

2.1. Ethics approval

All applicable international, national, and/or institutional guidelines for the care and use of animals were followed. We followed the laboratory animal guideline for the ethical review of the animal welfare of China (GB/T 35892–2018).

2.2. Animals

Red crucian carp (RCC, average length 15.1 ± 0.82 cm) was acclimatized in 70 × 65 × 65 cm plastic aquarium (25 fishes/aquarium) with the clean freshwater (pH 8.0, 23 ± 1 °C) for two weeks and fed with commercial diet twice daily till 24 h before challenge experiment, respectively. In addition, water quality was properly controlled to avoid pathogenic contamination during fish acclimation or immune challenge.

2.3. Immune challenge with A. hydrophila

A. hydrophila strain L3-3 (accession number: OM184261) was cultured in Luria-Bertani (LB) medium at 28 °C for 24 h, centrifuged at 10,000 ×*g* at 4 °C for 15 min and resuspended in 1 × PBS (pH 7.3) [18]. Then, fish receiving 100 μl suspension of 1×10^7 CFU ml^{-1} *A. hydrophila* in phosphate buffered saline (PBS) was served as infection group (RCCah), while injection of 100 μl sterile PBS was used as the control group (RCCctl). Kidney samples were isolated from RCC at 48 h post-infection. Each group contained six sets of kidney samples for biological replication. Each set was the single sample isolated from three different individuals.

2.4. Sample preparation for nontargeted metabolomics by liquid chromatography-mass spectrometry (LC-MS)

Sample preparation for LC-MS metabolomics was performed as previously described [19]. Following protein removal, filtrated samples were dried in vacuum and analyzed by ultraperformance liquid chromatography (UPLC) coupled to a premium quadrupole-time of flight mass spectrometer (QTOF-MS) [20]. Binary gradient elution system is composed of water (containing 0.1% formic acid, *v*/v) and acetonitrile (containing 0.1% formic acid, v/v). LC-MS metabolomics was operated in positive and negative ion mode (scan range 50–1000 *m/z*). QCs were injected at regular intervals throughout the analytical run.

2.5. LC-MS data processing and pathway analysis

Raw data were analyzed by progenesis QI software. Then, LC-MS data were shown with mass/charge ratio (*m/z*), peak retention time (RT) and peak intensity, while RT-m/z pairs were used for ion identification. Resulting matrix was reduced by peak removals with more than 60% missing value (ion intensity = 0) in samples. Internal standard was used for QC analysis and the metabolites were annotated by using public metabolic database, which were subjected to principal component analysis (PCA) and partial least squares discriminate analysis (PLS-DA). Threshold of variable importance in projection (VIP) was set to 1 for ranking metabolites. Differential metabolites were analyzed by hierarchical cluster analysis (HCA) and represented as heat map, which was performed on the log transformed normalized data and completed in R platform using distance matrix. Then, differential metabolites were analyzed by Kyoto Encyclopedia of Genes and Genomes (KEGG) database.

2.6. Histological analysis

Based on the protocols, kidney samples were fixed in Bouin solution, dehydrated in ethanol, clarified in xylene, and embedded in paraffin wax. After that, the samples were sectioned (approximately 5 μm thick) and stained by using a hematoxylin and eosin (HE) staining kit [21]. The prepared slides of the sections were examined by using a light microscope with 200× magnification. The experiment was repeated in triplicate.

2.7. Measurement of total superoxide dismutase (SOD) activity

According to protocols of total SOD activity kit (Beyotime Biotechnology, Shanghai, China), enzymatic activities in kidney were measured as the changes in absorbance at 560 nm. Results were given in units of SOD activity per milligram of protein, where 1 U of SOD is defined as the amount of enzyme producing 50% inhibition of SOD. The experiment was repeated in triplicate.

2.8. Measurement of catalase (CAT) activity

Based on protocols of catalase (CAT) activity kit (Nanjing Jiancheng Bioengineering Institute, Nanjing, China), reaction compounds could be monitored by the absorbance at 405 nm. Results were given in units of CAT activity per milligram of protein, where 1 U of CAT is defined as the amount of enzyme decomposing 1 μmol H_2O_2 per second. The experiment was repeated in triplicate.

2.9. Measurement of total antioxidant capacity (T-AOC)

Based on protocols of total antioxidant capacity (T-AOC) assay kit with ABTS method (Beyotime Biotechnology, Shanghai, China), T-AOC level in kidney was determined by the absorbance at 734 nm. Trolox solution was used as a reference standard. The experiment was repeated in triplicate.

2.10. Measurement of malondialdehyde (MDA) production

Free MDA and lipid hydroperoxides can be determined by thiobarbituric acid (TBA) method. According to protocols of lipid peroxidation MDA assay kit (Beyotime Biotechnology, Shanghai, China), tissue MDA amount was measured. The concentration of MDA was expressed as micromole MDA per milligram of protein. The experiment was repeated in triplicate.

2.11. Determination of glutathione peroxidase (GPx) activity

According to protocols of cellular glutathione peroxidase assay kit with NADPH (Beyotime Biotechnology, Shanghai, China), GPx activity in kidney was measured at 340 nm. Results were expressed as mU GPx activity per milligram of protein. The experiment was repeated in triplicate.

2.12. Determination of glutathione reductase (GR) activity

According to protocols of glutathione reductase assay kit with DTNB (Beyotime Biotechnology, Shanghai, China), GR activity in kidney was measured at 412 nm. Results were expressed as mU GR activity per milligram of protein. The experiment was repeated in triplicate.

2.13. Determination of NADPH/$NADP^+$ ratio

NADPH/$NADP^+$ contents in kidney were determined by using NADPH/$NADP^+$ assay kit (Beyotime Biotechnology, Shanghai, China). Then, NADPH/$NADP^+$ ratios were calculated as: [NADPH]/[$NADP^+$] = [NADPH] / ([NADP total] − [NADPH]). The experiment was repeated in

Table 1
The primer sequences used in this study.

Primer names	Sequence direction (5′ → 3′)	Use
RT-actin-F	GACCGAGCGTGGCTACAG	qPCR
RT-actin-R	GATACCGCAAGACTCCATACC	qPCR
RT-Bax-F	GGTGGAGGCGATACGGG	qPCR
RT-Bax-R	CGAGTTGGTTGAAGAGTGGAGT	qPCR
RT-caspase-3-F	AGATGCTGCTGAGGTCGGG	qPCR
RT-caspase-3-R	GGTCACCACGGGCAACTG	qPCR
RT-caspase-8-F	TGTGAATCTTCCAAAGGCAAA	qPCR
RT-caspase-8-R	CTGTATCCGCAACAACCGAG	qPCR
RT- HSP90α-F	AGCAGCCGATGATGGA	qPCR
RT- HSP90α-R	GGATTTGGCGATGGTTC	qPCR
RT-CA2-F	TGATGAATCGCTGAAACCG	qPCR
RT-CA2-R	GTCGTCGCTGGCACCC	qPCR
RT-STS-F	GGAAGGTGGGATTCGGAT	qPCR
RT-STS-R	ATGACTCTGTCGCTGGGTTT	qPCR
RT-17βHSD8-F	CATCACTGTGGGCAGCATAG	qPCR
RT-17βHSD8-R	GCTCTTTGGCAGCGGTT	qPCR
RT-BCL2-F	AGCCGCAGTATTGTGGTGA	qPCR
RT-BCL2-R	CATTTCCGCAAAGTCCGA	qPCR
RT-NR13-F	GGCTGGAGGAAAACGGAG	qPCR
RT-NR13-R	AACAGTGCGGTCTTCATCG	qPCR
RT-TrxR-F	TCCTGGGGTCTGGGTGG	qPCR
RT-TrxR-R	CAGCCGAACTTGCGTGC	qPCR
RT-CAT-F	ACCCATCGCTGTTCGTTTT	qPCR
RT-CAT-R	AGTTGCCCTCATCGGTGTAG	qPCR
RT-CuZnSOD-F	GGACCAACGGATAGCGACA	qPCR
RT-CuZnSOD-R	CCAGGCGACTTCCAGCG	qPCR
RT-MnSOD-F	CACTGCCTGACCTCCCAT	qPCR
RT-MnSOD-R	CCATCCTGAGCCCTGAAC	qPCR

triplicate.

2.14. Detection of ROS production

ROS content in kidney was measured by using DCFH-DA probe (Beyotime Biotechnology, Shanghai, China) as previously described [22]. In brief, the supernatants of 10% tissue homogenates were mixed with DCFH-DA probe. Then, reaction mixtures were measured by a fluorescence reader with an excitation wave length of 480 nm and emission wavelength of 520 nm. The experiment was repeated in triplicate.

2.15. RNA isolation and cDNA synthesis

Total RNA isolation and cDNA synthesis were performed as previously described [23]. In brief, total RNA was extracted from kidney samples by using HiPure Total RNA Mini kit (Magen, China). After that, concentration and integrity of purified total RNA were determined by measurement of 260/280 nm absorbance and agarose gel electrophoresis, respectively. 1000 ng of purified total RNA was used for cDNA synthesis using Revert AidTM M-MuLV Reverse Transcriptase Kit (MBI Fermentas, USA).

2.16. Quantitative real-time PCR (qRT-PCR) assay

Expression profiles of caspase-3, caspase-8, Bcl-2-associated X protein (Bax), Bcl-2 (B-cell lymphoma-2), anti-apoptotic protein NR13-like, heat shock protein 90 alpha (HSP90α), manganese-containing superoxide dismutase (MnSOD), copper zinc superoxide dismutase (CuZnSOD), thioredoxin reductase (TrxR), catalase (CAT), carbonic anhydrase 2 (CA2), steroid sulfatase (STS), hydroxysteroid 17-beta dehydrogenase 8, (17β-HSD8) were examined by using Applied Biosystems QuantStudio 5 Real-Time PCR System (Applied Biosystems, USA). At the end of qRT-PCR amplified reactions, melting curve analysis was implemented to confirm credibility of each qRT-PCR analysis. Expression of β-actin was measured and used as internal control to normalize results of qRT-PCR analyses. All primers were checked to be completely identical to sequences of target genes and primer specificity was confirmed prior to qRT-PCR assay. Each sample was analyzed in triplicate. The primers were shown in Table 1. qRT-PCR results were measured with $2^{-\Delta\Delta Ct}$ methods.

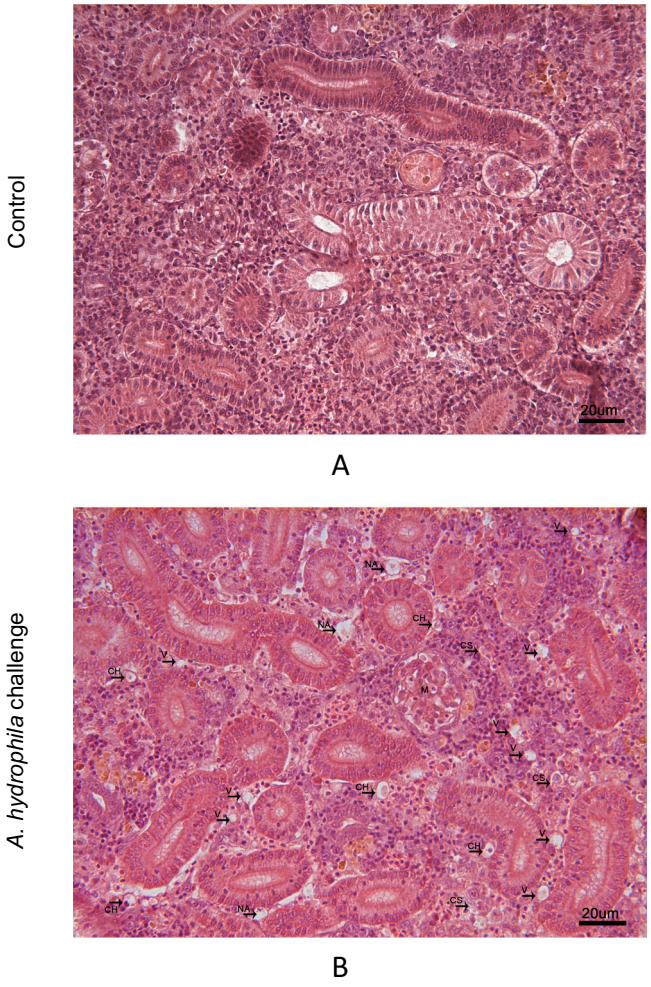

Fig. 1. Histological sections of kidney in RCC following *A. hydrophila* challenge. The control samples (A) and *A. hydrophila*-infected samples (B) were sectioned and stained by using a hematoxylin and eosin (HE) staining kit. CH: cell hypertrophy; NA: nuclear atrophy; CS: cloudy swelling; V: vacuolization; M: mesangial cells.

2.17. Statistical analyses

The data analyses were measured by using SPSS 18 analysis program and represented as means ± standard deviation. All of the experimental data analyses were subjected to Student's *t*-test or one-way ANOVA (one-way analysis of variance). Further analysis of Duncan's multiple range test, only if the level of *P*-value <0.05, the differences were considered statistically significant.

3. Results

3.1. Tissue damage and antioxidant status in kidney following *A. hydrophila* challenge

As shown in Fig. 1A-B, *A. hydrophila* challenge could stimulate ranges of tissue damage in kidney of RCC, including cell hypertrophy, cytoplasmic vacuolation, nuclear atrophy, cloudy swelling and formation of mesangial cells.

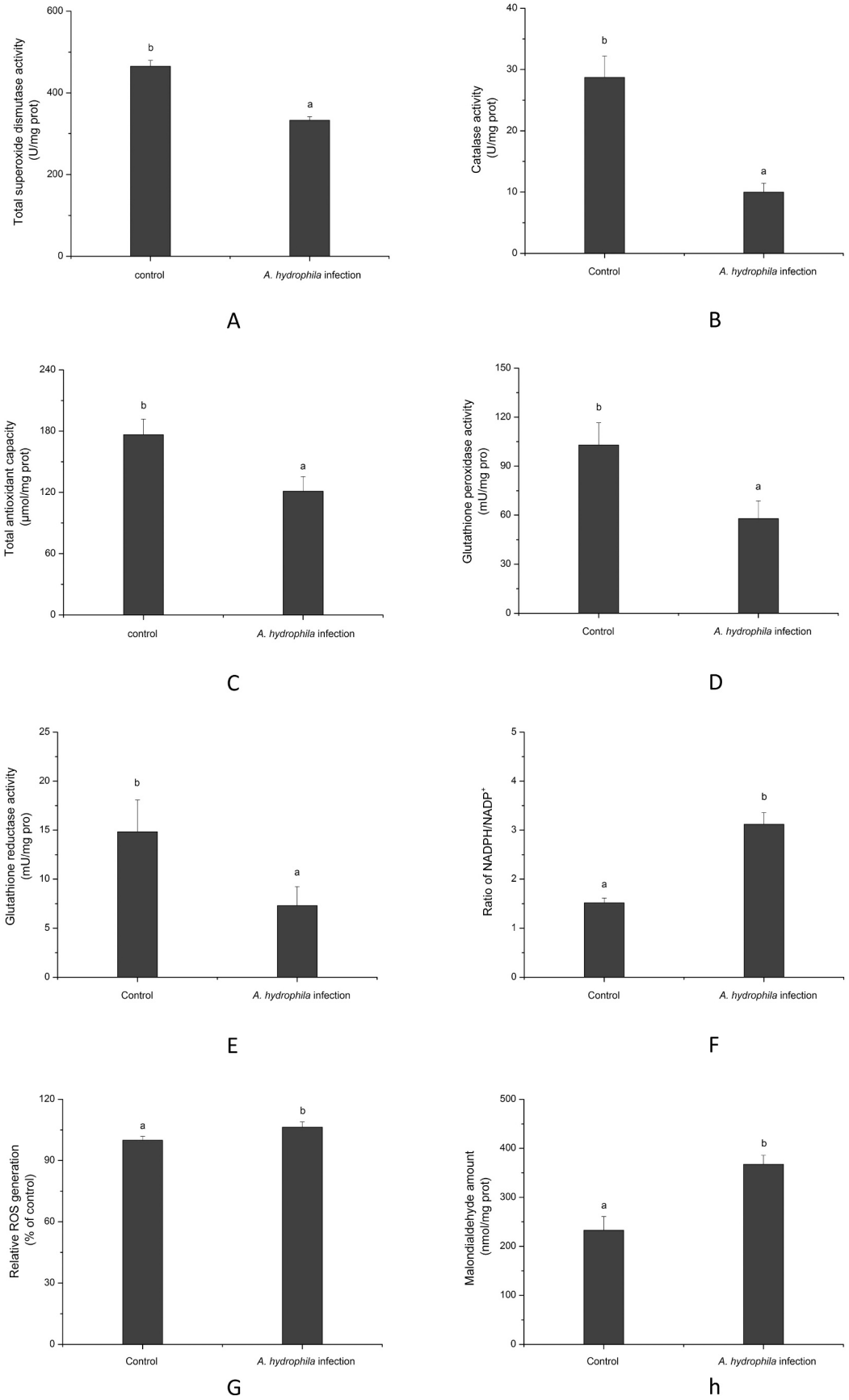

Fig. 2. Antioxidant status in kidney of RCC after *A. hydrophila* challenge. Total SOD (A), CAT (B), T-AOC (C), GPx (D), GR (E), NADPH/$NADP^+$ ratio (F), ROS generation (G) and MDA (H) were measured by a microplate reader. The calculated data (mean ± SD) with different letters were significantly different ($P < 0.05$).

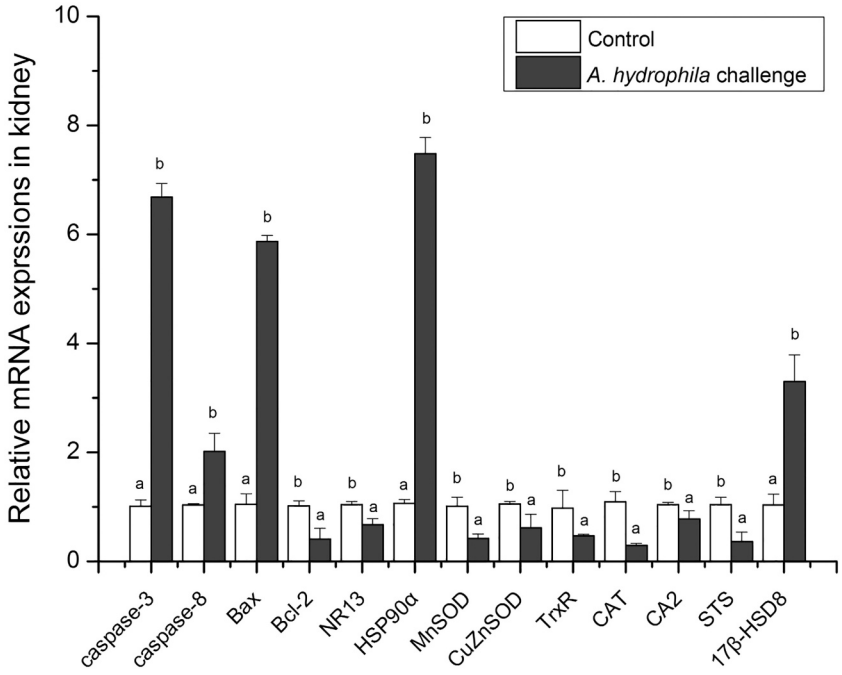

Fig. 3. Gene expression profiles in kidney of RCC following *A. hydrophila* challenge. Relative expressions of caspase-3, caspase-8, Bax, HSP90α, 17β-HSD8, Bcl-2, NR13, MnSOD, CuZnSOD, TrxR, CAT, CA2 and STS in kidney of RCC were calculated by the $2^{-\Delta\Delta Ct}$ methods. The calculated data (mean ± SD) with different letters were significantly different ($P < 0.05$).

Antioxidant parameters in kidney following *A. hydrophila* challenge were shown in Fig. 2A-H. Total SOD activity, CAT activity, GPx activity, GR activity and T-AOC level decreased sharply after *A. hydrophila* challenge, whereas a significant increase of NADPH/$NADP^+$ ratio, ROS production and MDA amount was detected.

3.2. Gene expressions determined by qRT-PCR assay

In Fig. 3, expression profiles of oxidative stress indicators, apoptotic genes and metabolic enzyme genes were investigated following *A. hydrophila* infection. Expression levels of caspase-3, caspase-8, Bax, HSP90α, and 17β-HSD8 increased significantly in RCC subjected to *A. hydrophila* challenge, while a sharp decrease of Bcl-2, NR13, MnSOD, CuZnSOD, TrxR, CAT, CA2 and STS mRNA was detected.

3.3. Metabolite categories and profiles after A. hydrophila infection

In order to obtain clear separation of LC-MS metabolic data from control samples and *A. hydrophila* infection samples, combination analysis of PCA model and PLS-DA model was investigated in this study. The scatter plot of PCA model obtained with data of kidney samples was shown in Fig. 4A. The cross-validation of predicted model showed a PC1 value of 26.02% for the first component and a PC2 value of 21.26% for the second component. Furthermore, LC-MS data were analyzed by PLS-DA model. The predicted model showed a PC1 value of 25.05% for the first component and a PC2 value of 6.87% for the second component, which is subjected to permutation test (Fig. 4B-C). To characterize crucial metabolic biomarkers in RCC after *A. hydrophila* infection, secondary metabolites were analyzed based on metabolomics database. In Fig. 5A, percentages of metabolic categories in RCCah vs RCCctl ranked amino acids > lipids > carbon sources = nucleotides. In Fig. 5B-C, a total of 244 differential metabolites were detected in RCCah vs RCCctl, containing 66 increased metabolites and 178 decreased metabolites. The numbers of increased and decreased metabolites in RCCah vs RCCctl were shown in Fig. 5D. Most numbers of metabolites in amino acids, carbon sources and lipids were down-regulated in RCCah vs RCCctl, while most numbers of metabolites in nucleotides were up-regulated.

To represent the relative contents of crucial metabolites (*P*-value < 0.05, VIP ≥ 1) in RCCah vs RCCctl, HCA-heatmap of top 60 metabolites were investigated. As shown in Fig. 6, relative abundances of most stress-induced hormones increased dramatically in RCCah vs RCCctl, while the contents of phosphatidylcholine (PC), lysophosphatidylcholine (LysoPC), lysophosphatidylethanolamine (LysoPE), lysophosphatidylinositol (LysoPI) and various dipeptides were significantly down-regulated.

3.4. Important metabolites and pathway analysis

To investigate the mechanisms linking *A. hydrophila*-induced metabolites in RCC and the specific pathways, the obtained secondary metabolites were used for pathway enrichment by KEGG analysis. In Fig. 7A, differential metabolites in RCCah vs RCCctl belonged to five main categories, including “Cellular processes”, “Environmental information processing”, “Genetic information processing”, “Metabolism” and “Organismal systems”, while the most assigned category was “Metabolism”. In Fig. 7B, “Bile secretion” and “Steroid hormone biosynthesis” enriched the most metabolites in RCCah vs RCCctl, while “Bile secretion” was significantly enriched. Based on VIP scores analysis, the crucial metabolites determined from “Bile secretion” and “Steroid hormone biosynthesis” were shown in Fig. 7C. Thirteen metabolites were determined as the crucial metabolite indicators, while the stress-induced hormones such as choline, tetrahydrocortisone, spermine, cortisol and estrone (VIP > 1.5) may appear to play important roles in metabolic processes of RCC subjected to *A. hydrophila* infection.

4. Discussion

A. hydrophila is a gram-negative bacteria that can cause severe disease outbreak during aquaculture. Among known secreted virulent factors, aerolysin can promote cell hemolysis and cause deep wound infection by binding to specific glycophosphatidylinositol (GPI)-anchored proteins on the surface of fish cells [24]. In this study, we found that *A. hydrophila* challenge could stimulate ranges of tissue damage in kidney of RCC.

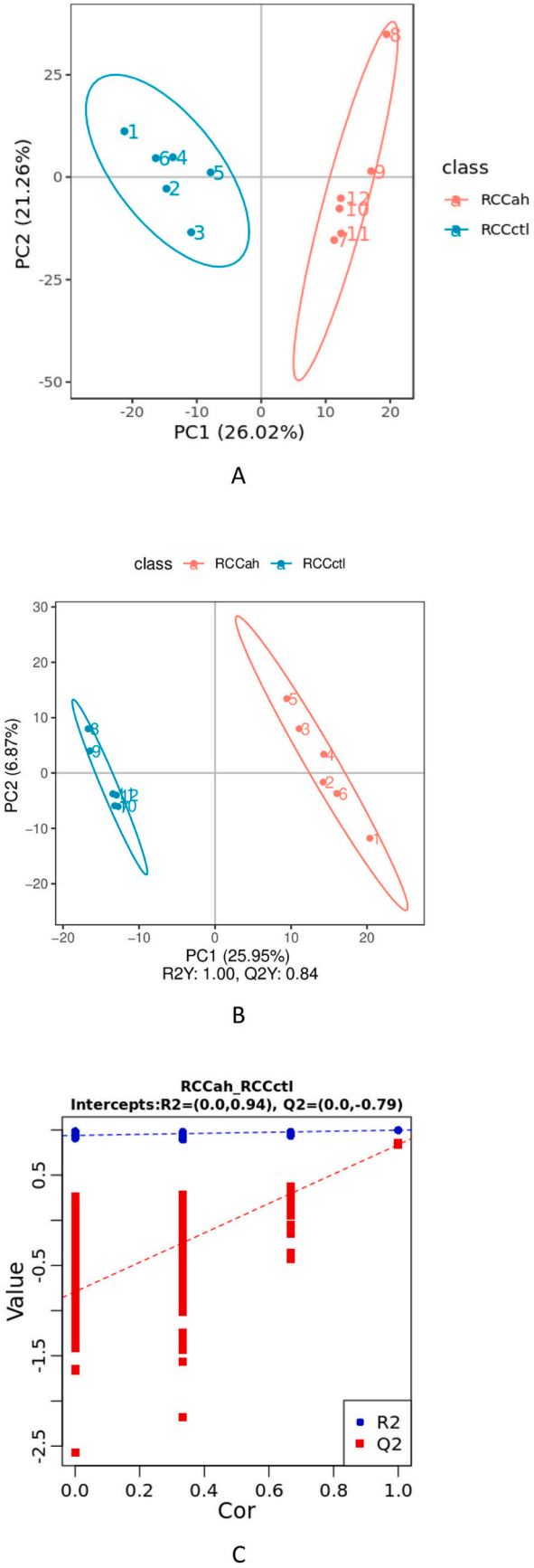

Fig. 4. PCA (A), PLS-DA analysis (B) and permutation plot analysis (C) of kidney samples showing separation of the experimental groups.

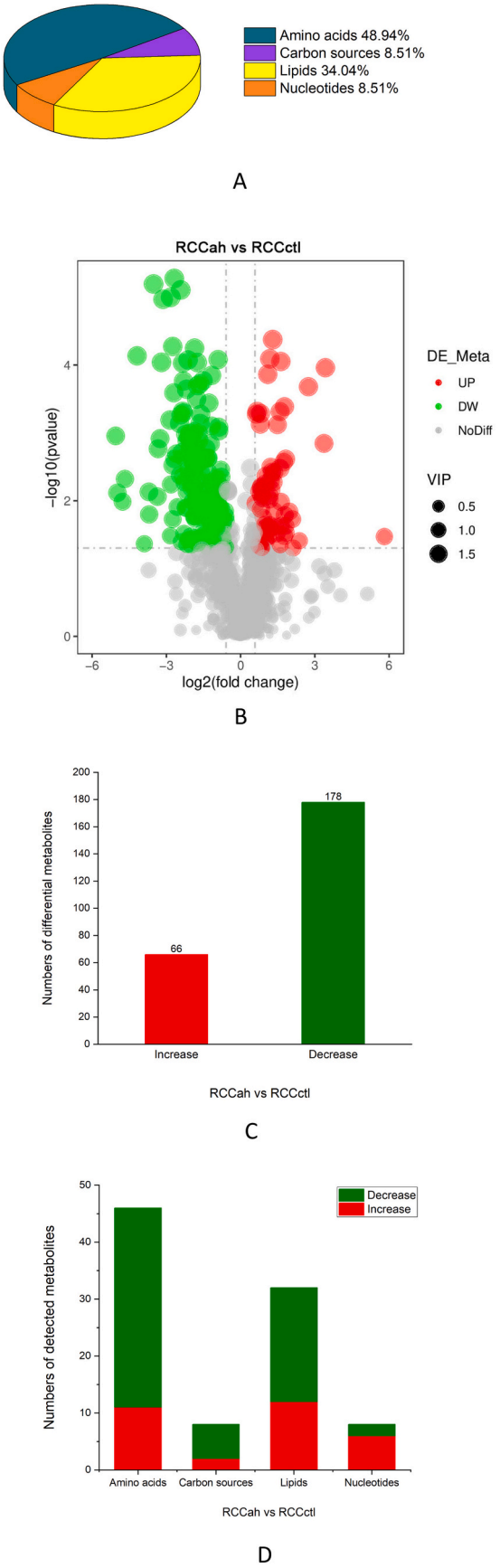

Fig. 5. Features of differential metabolites. (A) Percentage of differential metabolites of RCCah vs RCCctl in four categories. (B-D) Numbers of decreased and increased metabolites in RCCah vs RCCctl.

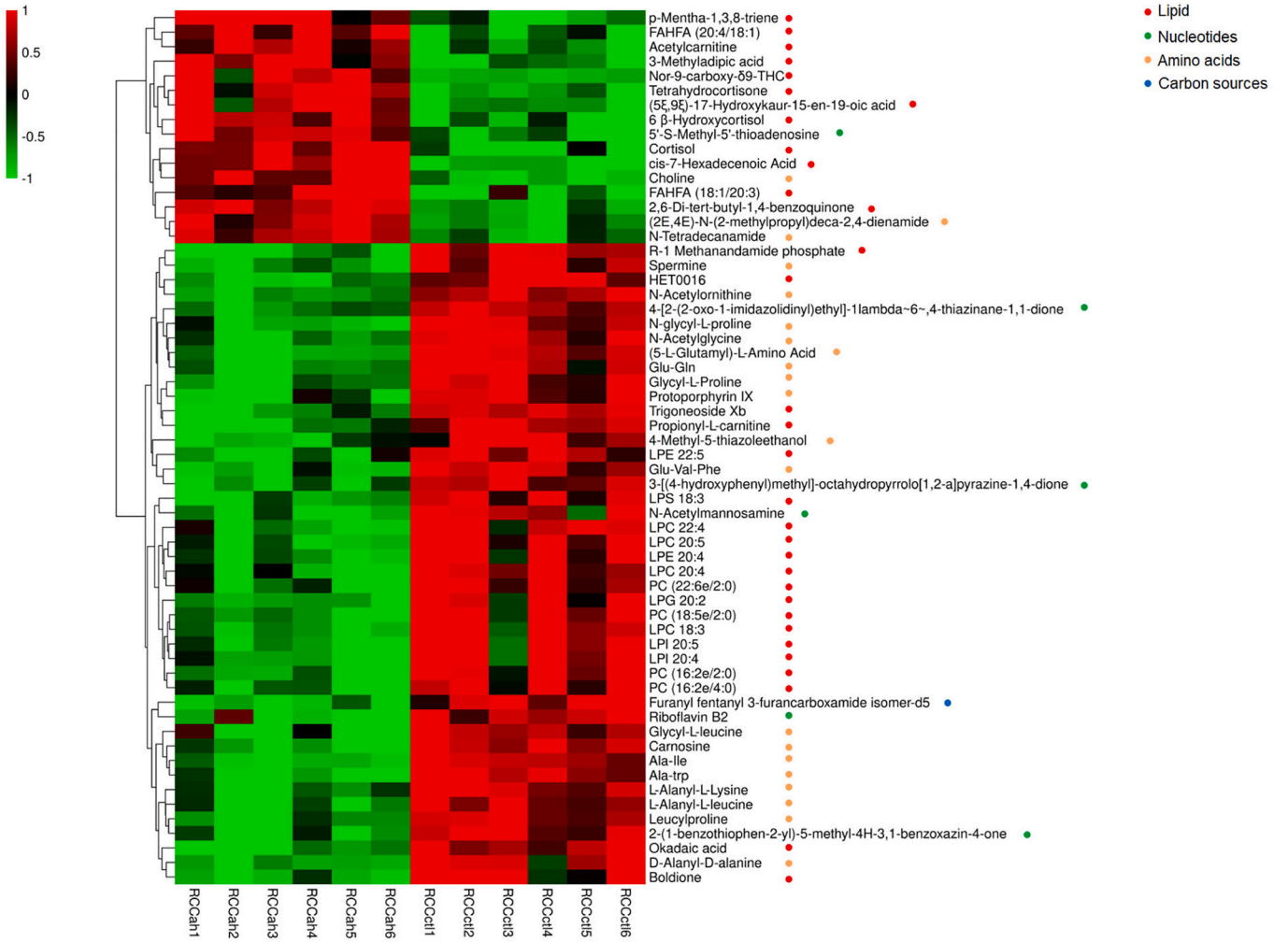

Fig. 6. HCA-heatmap showing the relative contents and relationship of top 60 metabolites (P-value < 0.05, VIP ≥ 1) in RCCah vs RCCctl.

In general, kidney is one of the major lymphoid tissues in fish, which is involved in lymphocytes- and macrophages-mediated immune response [25]. However, acute bacterial infection can induce oxidative stress, resulting in redox imbalance and lipid peroxidation [26]. Additionally, excessive accumulation of intracellular ROS may impair host immunity, affect metabolic response and delay bacterial clearance [27]. Although antioxidant enzymes and compounds can alleviate cytokine-mediated toxicity [28], severe oxidative stress can attenuate antioxidant defense in fish [29]. In this study, decreased levels of total SOD activity, CAT activity, GPx activity, GR activity and T-AOC level along with up-regulation of NADPH/$NADP^+$ ratio, ROS production and MDA amount were observed in kidney following *A. hydrophila* challenge. In addition, down-regulated expressions of MnSOD, CuZnSOD, TrxR and CAT along with increased levels of HSP90α were observed in kidney following *A. hydrophila* challenge. These results implied that acute *A. hydrophila* infection could significantly suppress antioxidant defense in RCC undergoing severe oxidative stress.

Evidences are emerging that mitochondrial malfunction is highly associated with increased level of intracellular oxidative stress, which is considered as an early event in apoptosis [30,31]. Apoptosis is highly modulated cell death process in the normal development and homeostasis within the host that can mitigate autoimmunity and ameliorate aberrant immune response, as well as remodel inflamed sites via phagocytic clearance of dying cells [32]. The expression ratios of pro-apoptotic and anti-apoptotic genes may delineate apoptotic status in cells and then determinate cell survive and death [33]. In this study, pro-apoptotic genes (caspase-3, caspase-8 and Bax) and anti-apoptotic genes (Bcl-2 and NR13) were investigated in kidney after *A. hydrophila* infection. Enhanced levels of caspase-3, caspase-8 and Bax along with decreased expressions of Bcl-2 and NR13, suggesting that *A. hydrophila* infection could augment the activation of apoptotic signals in kidney of RCC.

Exposure to stressors may alter teleostean non-specific response in hormone levels, metabolite contents, hydromineral balance and hematological changes, which may enable fish to maintain homeostasis and counteract stress-evoked adverse effects [34]. Previous findings indicate that *Salmonella* infection elicits a profound effect on tissue metabolite profiles, disturbing eicosanoid metabolism, steroid metabolism and bile acid synthesis [35]. In this study, LC-MS results analyzed by KEGG revealed that *A. hydrophila* infection could significantly alter amino acid metabolism and lipid metabolism in kidney of RCC, whereas the most metabolites were enriched in bile secretion and steroid hormone biosynthesis. In addition, transcript levels of CA2 and STS decreased significantly in kidney following *A. hydrophila* challenge, while 17β-HSD8 expression increased sharply. As is well known, amino acids can serve as preferential energetic substrates together with fatty acids, while its deficiency may damage immune function and enhance the susceptibility to infectious diseases [36]. Fatty acids are not only important energy sources metabolized by β-oxidation, but also function as signal molecules that can regulate various cellular processes and physiological functions [37]. In general, bile contains complex components, including bile salt, fatty acid, cholesterol and bicarbonate, while CA2 expression

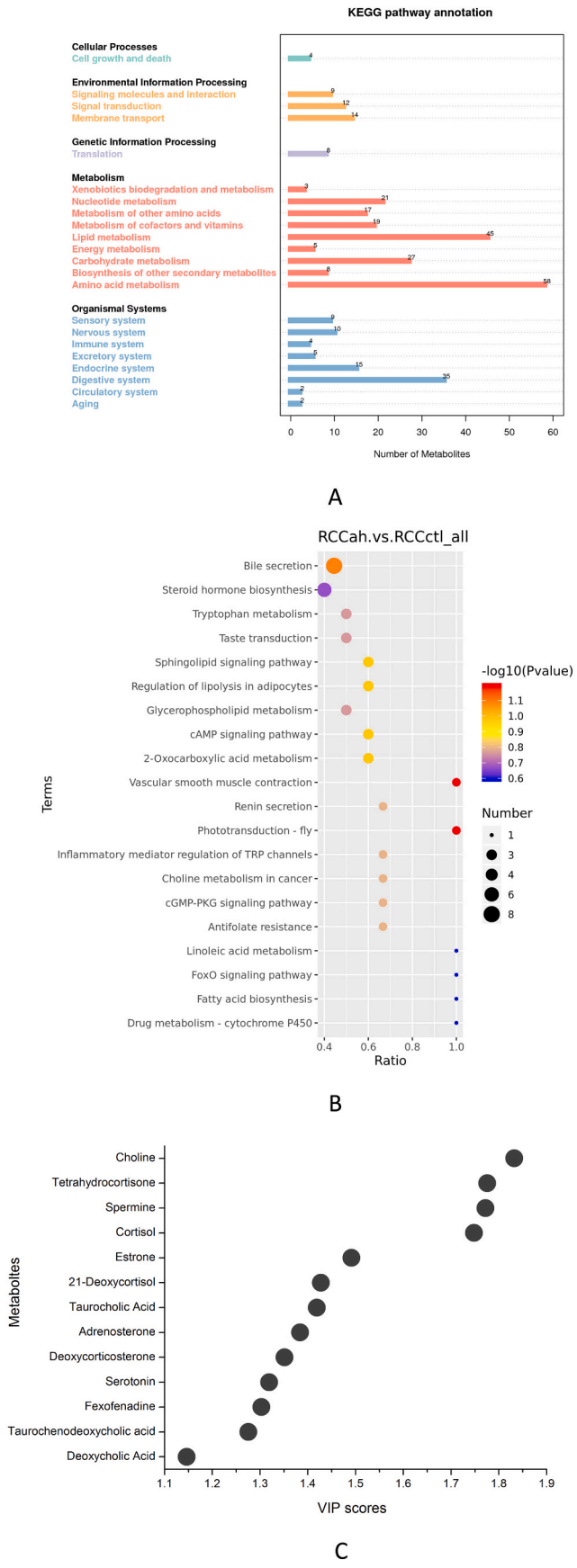

Fig. 7. KEGG analysis and crucial metabolites in RCCah vs RCCctl. (A) KEGG annotation of detected metabolites in RCCah vs RCCctl. (B) KEGG pathway of detected metabolites in RCCah vs RCCctl. (C) VIP scores of crucial metabolites.

may be involved in the production of bicarbonate for its further secretion to bile [38]. Bile secretion plays an important role in the lipid digestion and absorption, but invading bacteria may resist bactericidal conditions of bile and utilize bile as a key signal molecule to enhance their virulence regulation for efficient infection [39]. In addition, pathogenic infection may also enhance bile acid deconjugation, elevate energy expenditure and dysregulate lipid metabolism, causing growth impairment [40]. In addition, both 17β-HSD isozymes and STS play vital roles in steroid hormone metabolism and formation of biologically active steroids [41,42]. Steroid hormones not only elicit a profound effect in maintenance of host metabolic homeostasis, but also participate in generating antimicrobial peptides [43] and antagonizing toxin-induced pathopysiological levels of inflammatory response [44]. In turn, invading bacteria could alter steroid synthesis and metabolism, receptor signal activities and expressions of genes containing hormone response elements [45]. Thus, taken together, *A. hydrophila* challenge exhibited a profound effect on amino acid metabolism and lipid metabolism, dramatically decreasing dipeptide and fatty acid derivatives along with elevated levels of stress-induced hormones in kidney of RCC.

In summary, we characterized histological analysis, antioxidant activities, apoptotic gene expressions and metabolic features in RCC following *A. hydrophila* challenge. Our findings revealed that *A. hydrophila* infection could induce kidney injury, decrease antioxidant status along with increased level of apoptotic processes. In addition, we further identified dipeptides, fatty acid derivatives, cortisol, choline and tetrahydrocortisone as crucial biomarkers in kidney of RCC subjected to *A. hydrophila* challenge. Thus, the information presented in this study could highlight the importance of metabolic strategy to cope with bacterial infection.

Declaration of competing interest

The authors declare that they have no conflict of interest.

Acknowledgements

This research was supported by the National Natural Science Foundation of China, China (grant no. 31902363) and Hunan Provincial Natural Science Foundation, China (grant no. 2021JJ40340).

References

1 Qi, Z., Zhang, Y., Chen, Z.-F., Yang, C., Song, Y., Liao, X., et al., 2020. Chemical identity and cardiovascular toxicity of hydrophobic organic components in PM2. 5, 201, 110827.
2 Magnadottir, B., 2010. Immunological control of fish diseases. Mar. Biotechnol. 12, 361–379.
3 Yang, C., Liu, L., Liu, J., Ye, Z., Wu, H., Feng, P., et al., 2019. Black carp IRF5 interacts with TBK1 to trigger cell death following viral infection. Dev. Comp. Immunol. 100, 103426.
4 Martinez, J.L., 2009. Environmental pollution by antibiotics and by antibiotic resistance determinants. Environ. Pollut. 157, 2893–2902.
5 Nascimento, A.M., Chartone-Souza, E., 2003. Operon mer: bacterial resistance to mercury and potential for bioremediation of contaminated environments. Genet. Mol. Res. 2, 92–101.
6 Rodger, H.D., 2016. Fish disease causing economic impact in global aquaculture. In: Fish Vaccines. Springer, pp. 1–34.
7 Li, Z., Wang, Z.W., Wang, Y., Gui, J.F., 2018. Crucian carp and gibel carp culture. In: Aquaculture in China: Success Stories and Modern Trends, pp. 149–157.
8 Nielsen, M.E., Høi, L., Schmidt, A., Qian, D., Shimada, T., Shen, J., et al., 2001. Is Aeromonas hydrophila the dominant motile Aeromonas species that causes disease outbreaks in aquaculture production in the Zhejiang Province of China? Dis. Aquat. Org. 46, 23–29.
9 Secombes, C., Wang, T., Hong, S., Peddie, S., Crampe, M., Laing, K., et al., 2001. Cytokines and innate immunity of fish. Dev. Comp. Immunol. 25, 713–723.
10 Ellis, A., 1999. Immunity to bacteria in fish. Fish Shellfish Immunol. 9, 291–308.
11 Luo, S.-W., Kang, H., Xie, R.-C., Wei, W., Liang, Q.-j., Liu, Y., et al., 2019. N-terminal domain of EcC1INH in Epinephelus coioides can antagonize the LPS-stimulated inflammatory response. Fish Shellfish Immunol. 84, 8–19.
12 Wilhelm, Filho D., 2007. Reactive oxygen species, antioxidants and fish mitochondria. Front. Biosci. 12, 1229–1237.
13 Daskalov, H., 2006. The importance of Aeromonas hydrophila in food safety. Food Control 17, 474–483.

14 Liu, B., Xu, L., Ge, X., Xie, J., Xu, P., Zhou, Q., et al., 2013. Effects of mannan oligosaccharide on the physiological responses, HSP70 gene expression and disease resistance of Allogynogenetic crucian carp (Carassius auratus gibelio) under Aeromonas hydrophila infection. Fish Shellfish Immunol. 34, 1395–1403.
15 Gudding, R., Van Muiswinkel, W.B., 2013. A history of fish vaccination: science-based disease prevention in aquaculture. Fish Shellfish Immunol. 35, 1683–1688.
16 Dong, H., Chen, Y., Wang, J., Zhang, Y., Zhang, P., Li, X., et al., 2020. Interactions of microplastics and antibiotic resistance genes and their effects on the aquaculture environments. J. Hazard. Mater. 123961.
17 Lercher, A., Baazim, H., Bergthaler, A., 2020. Systemic immunometabolism: challenges and opportunities. Immunity 53, 496–509.
18 Xiong, N.-X., Ou, J., Li, S.-Y., Zhao, J.-H., Huang, J.-F., Li, K.-X., et al., 2022. A novel ferritin L (FerL) in hybrid crucian carp could participate in host defense against Aeromonas hydrophila infection and diminish inflammatory signals. Fish Shellfish Immunol. 120, 620–632.
19 Naz, S., Moreira dos Santos, D.C., García, A., Barbas, C., 2014. Analytical protocols based on LC–MS, GC–MS and CE–MS for nontargeted metabolomics of biological tissues. Bioanalysis 6, 1657–1677.
20 Pekkinen, J., Olli, K., Huotari, A., Tiihonen, K., Keski-Rahkonen, P., Lehtonen, M., et al., 2013. Betaine supplementation causes increase in carnitine metabolites in the muscle and liver of mice fed a high-fat diet as studied by nontargeted LC-MS metabolomics approach. Mol. Nutr. Food Res. 57, 1959–1968.
21 Song, X., Zhao, J., Bo, Y., Liu, Z., Wu, K., Gong, C., 2014. Aeromonas hydrophila induces intestinal inflammation in grass carp (Ctenopharyngodon idella): an experimental model. Aquaculture 434, 171–178.
22 Ma, P., Yan, B., Zeng, Q., Liu, X., Wu, Y., Jiao, M., et al., 2014. Oral exposure of Kunming mice to diisononyl phthalate induces hepatic and renal tissue injury through the accumulation of ROS. Protective effect of melatonin. Food Chem. Toxicol. 68, 247–256.
23 Xiong, N.-X., Ou, J., Fan, L.-F., Kuang, X.-Y., Fang, Z.-X., Luo, S.-W., et al., 2022. Blood cell characterization and transcriptome analysis reveal distinct immune response and host resistance of different ploidy cyprinid fish following Aeromonas hydrophila infection. Fish Shellfish Immunol. 120, 547–559.
24 Singh, V., Somvanshi, P., Rathore, G., Kapoor, D., Mishra, B., 2010. Gene cloning, expression, and characterization of recombinant aerolysin from Aeromonas hydrophila. Appl. Biochem. Biotechnol. 160, 1985–1991.
25 Press, C.M., Evensen, Ø., 1999. The morphology of the immune system in teleost fishes. Fish Shellfish Immunol. 9, 309–318.
26 Lesser, M.P., 2006. Oxidative stress in marine environments: biochemistry and physiological ecology. Annu. Rev. Physiol. 68, 253–278.
27 Su, Y.-C., Jalalvand, F., Thegerström, J., Riesbeck, K., 2018. The interplay between immune response and bacterial infection in COPD: focus upon non-typeable haemophilus influenzae. Front. Immunol. 9, 2530.
28 Lortz, S., Tiedge, M., Nachtwey, T., Karlsen, A.E., Nerup, J., Lenzen, S., 2000. Protection of insulin-producing RINm5F cells against cytokine-mediated toxicity through overexpression of antioxidant enzymes. Diabetes 49, 1123–1130.
29 Xiong, N.-X., Luo, S.-W., Mao, Z.-W., Fan, L.-F., Luo, K.-K., Wang, S., et al., 2021. Ferritin H can counteract inflammatory response in hybrid fish and its parental species after Aeromonas hydrophila infection.
30 Ly, J.D., Grubb, D., Lawen, A., 2003. The mitochondrial membrane potential (Δψm) in apoptosis; an update. Apoptosis 8, 115–128.
31 Luo, S.-W., Xiong, N.-X., Luo, Z.-Y., Luo, K.-K., Liu, S.-J., Wu, C., et al., 2021. Effect of lipopolysaccharide (LPS) stimulation on apoptotic process and oxidative stress in fibroblast cell of hybrid crucian carp compared with those of Carassius cuvieri and Carassius auratus red var. Comp. Biochem. Physiol. C: Toxicol. Pharmacol. 248, 109085.
32 Savill, J., 1997. Apoptosis in resolution of inflammation. J. Leukoc. Biol. 61, 375–380.
33 Akbar, A.N., Borthwick, N.J., Wickremasinghe, R.G., Panayiotidis, P., Pilling, D., Bofill, M., et al., 1996. Interleukin-2 receptor common γ-chain signaling cytokines regulate activated T cell apoptosis in response to growth factor withdrawal: selective induction of anti-apoptotic (bcl-2, bcl-xL) but not pro-apoptotic (bax, bcl-xS) gene expression. Eur. J. Immunol. 26, 294–299.
34 Barton, B.A., 2002. Stress in fishes: a diversity of responses with particular reference to changes in circulating corticosteroids. Integr. Comp. Biol. 42, 517–525.
35 Antunes, L.C.M., Arena, E.T., Menendez, A., Han, J., Ferreira, R.B., Buckner, M.M., et al., 2011. Impact of salmonella infection on host hormone metabolism revealed by metabolomics. Infect. Immun. 79, 1759–1769.
36 Li, P., Yin, Y.-L., Li, D., Kim, S.W., Wu, G., 2007. Amino acids and immune function. Br. J. Nutr. 98, 237–252.
37 Kimura, I., Ichimura, A., Ohue-Kitano, R., Igarashi, M., 2019. Free fatty acid receptors in health and disease. Physiol. Rev. 100, 171–210.
38 Kivelä, A.J., Kivelä, J., Saarnio, J., Parkkila, S., 2005. Carbonic anhydrases in normal gastrointestinal tract and gastrointestinal tumours. World J. Gastroenterol 11, 155.
39 Sistrunk, J.R., Nickerson, K.P., Chanin, R.B., Rasko, D.A., Faherty, C.S., 2016. Survival of the fittest: how bacterial pathogens utilize bile to enhance infection. Clin. Microbiol. Rev. 29, 819–836.
40 Riba, A., Hassani, K., Walker, A., van Best, N., von Zeschwitz, D., Anslinger, T., et al., 2020. Disturbed gut microbiota and bile homeostasis in Giardia-infected mice contributes to metabolic dysregulation and growth impairment. Sci. Transl. Med. 12.
41 Reed, M., Purohit, A., Woo, L.L., Newman, S.P., Potter, B.V., 2005. Steroid sulfatase: molecular biology, regulation, and inhibition. Endocr. Rev. 26, 171–202.
42 Atanassova, N., Koeva, Y., 2012. Hydrohysteroid dehydrogenases–biological role and clinical importance–review. Dehydrogenases 115.
43 Marin-Luevano, S.P., Rodriguez-Carlos, A., Jacobo-Delgado, Y., Valdez-Miramontes, C., Enciso-Moreno, J.A., Rivas-Santiago, B., 2021. Steroid hormone modulates the production of cathelicidin and human β-defensins in lung epithelial cells and macrophages promoting Mycobacterium tuberculosis killing. Tuberculosis 128, 102080.
44 Ben-Nathan, D., Padgett, D.A., Loria, R.M., 1999. Androstenediol and dehydroepiandrosterone protect mice against lethal bacterial infections and lipopolysaccharide toxicity. J. Med. Microbiol. 48, 425–431.
45 Vom Steeg, L.G., Klein, S.L., 2017. Sex steroids mediate bidirectional interactions between hosts and microbes. Horm. Behav. 88, 45–51.